

More on Phase Transition and Rényi Entropy

Ahmad Ghodsi ^{*}and Saeed Qolibikloo [†]

*Department of Physics, Faculty of Science,
Ferdowsi University of Mashhad,
Mashhad, Iran*

November 14, 2018

Abstract

In this paper we study the scalar field condensation around the hyperbolic black hole solutions in Einstein and Gauss-Bonnet gravities. We investigate Rényi entropy and the inequalities governing on it under this phase transition. Our numerical computations show that for positive values of Gauss-Bonnet coupling and below the critical temperature one of these inequalities is violated. This puts more restriction on the allowed values of Gauss-Bonnet coupling.

arXiv:1811.04980v1 [hep-th] 12 Nov 2018

^{*}a-ghodsi@ferdowsi.um.ac.ir

[†]s.qolibikloo@mail.um.ac.ir

1 Introduction

Study of Entanglement Entropy (EE) has been a significant subject in recent years. As an evidence to its importance, one could point to its numerous applications in quantum information theory and quantum computation [1], condensed matter physics [2–5], quantum gravity and specially in holography [6–14].

Generally speaking, EE is a measure for degree of entanglement between two parts of a system in a given quantum state. To define it more carefully, consider a quantum system composed of two subsystems, A and its complement A^c , whose state can be described by a density matrix ρ . The entangling surface ∂A is defined as a boundary surface of the spatial region A in the quantum field theory (QFT) under consideration.

By tracing over the degrees of freedom in A^c , one can construct a reduced density matrix $\rho_A = \text{tr}_{A^c} \rho$. The EE between these two subsystems is measured by Von Neumann entropy of the reduced density matrix *i.e.* $S_{EE} = -\text{tr} \rho_A \log \rho_A$. The computation of $\log \rho_A$ is a hard task even in the simplest cases of two dimensional QFTs. Instead, one can compute $\text{tr} \rho_A^n$ and use it in the definition of Entanglement Rényi Entropy (ERE) [15]

$$S_n = \frac{1}{(1-n)} \log \text{tr} \rho_A^n. \quad (1.1)$$

Taking the limit $n \rightarrow 1$ one recovers the entanglement entropy *i.e.* $S_{EE} = \lim_{n \rightarrow 1} S_n$.

ERE contains many useful information about the spectrum of ρ_A . Indeed, one can recover the whole spectrum of the reduced density matrix ρ_A only by knowing the Rényi entropies for all integers $n > 0$ [16]. In particular, $S_\infty = -\log \lambda_{max}$, where λ_{max} is the largest eigenvalue of ρ_A . Another interesting case is $S_0 = \log D$, in which, D is the number of non-vanishing eigenvalues of ρ_A . And finally $S_2 = -\log \text{tr} \rho_A^2 = -\ln P$, where P is the probability of finding two systems in the same state, described by ρ_A after measurement in a diagonalized basis. These special cases are called min-entropy, Hartley or max-entropy and collision entropy respectively.

As we mentioned, the computation of $\text{tr} \rho_A^n$ is much easier than the computation of $\text{tr} \log \rho_A$. In the context of Conformal Field Theories (CFT)s, a standard way to calculate $\text{tr} \rho_A^n$ (and consequently S_{EE}) is the “Replica Trick”. In this method, after a Wick rotation from the flat Minkowski metric where the CFT lives to a metric with Euclidean signature, the desired $\text{tr} \rho_A^n$ operator is given in terms of the path integral on an n -sheeted Riemann surface

$$\text{tr} \rho_A^n = \frac{Z_n}{(Z)^n}, \quad (1.2)$$

where Z is the partition function of the original space-time and Z_n is the partition function on a singular space which is constructed by gluing n copies of the original space along the boundary ∂A . At the end $\text{tr} \rho_A^n$ essentially becomes the product of two point functions of twisted vertex operators [2, 17] which is very hard to calculate, except in very specific cases, for example see [18–20] or [8] and references therein. In any case, after computation of $\text{tr} \rho_A^n$, we can substitute it in the following equation to compute S_{EE} ,

$$S_{EE} = -\frac{\partial}{\partial n} \log \text{tr} \rho_A^n \Big|_{n=1}. \quad (1.3)$$

In the context of holography, EE was first appeared in [6] where the authors, Ryu and Takayanagi (RT), gave a simple yet ingenious way for the computation of S_{EE} . In their

method, the EE between two spatial regions A and its complement in the d -dimensional boundary CFT, is found to be proportional to the extremum of surface area of the bulk hypersurfaces Σ , which are homologous to the region A , *i.e.* $\partial A = \partial \Sigma$.

$$S_{EE}(A) = \text{Ext} \left[\frac{\mathcal{A}(\Sigma)}{4G_N} \right]. \quad (1.4)$$

The resemblance between the formula above and the Bekenstein-Hawking formula for black hole (BH) thermal entropy $S_{BH} = \frac{A}{4G}$, is extraordinary. However, the surface Σ does not need to coincide with any BH event horizon in general. This striking similarity prompted physicists to look for a derivation of the RT conjecture.

In paper [21] authors give a novel method for computation of entanglement entropy of a Spherical Entangling Surfaces (SES) in a CFT, on a flat Minkowski space-time. In what follows we will give a quick review of this approach.

First, let us consider a quantum system in a d -dimensional flat Minkowski space-time $R^{1,d-1}$, which is divided into two subsystems, A and its complement A^c . The subsystem A consists of a spatial region inside a ball of radius R , whose boundary (at time $t = 0$) is denoted by ∂A . The subsystem A can be described by a reduced density matrix $\rho_A = \text{tr}_{A^c} \rho$, where ρ is the density matrix of the vacuum state of the whole system. The Cauchy development, $D(A)$, of the region A by definition is the set of all space-time events $p \in R^{1,d-1}$ through which, every non space-like curve intersects A at least once. After a Wick rotation the metric is

$$ds_{R^d}^2 = dt_E^2 + dr^2 + r^2 d\Omega_{d-2}^2, \quad (1.5)$$

where t_E is the Euclidean time, r is the radial coordinate on the constant time slice ($t_E = 0$) and $d\Omega_{d-2}^2$ is the metric on a unit $(d-2)$ -sphere. Notice that SES in this metric is the region $(t_E, r) = (0, R)$. After a series of coordinate transformations (first $z = r + it_E$, second $\exp(-w) = \frac{R-z}{R+z}$ and finally $w = u + \frac{i\tau_E}{R}$) the metric can be written as

$$ds_{S^1 \times H^{d-1}}^2 = \Omega^2 ds_{R^d}^2 = d\tau_E^2 + R^2 (du^2 + \sinh^2 u d\Omega_{d-2}^2) = d\tau_E^2 + R^2 d\Sigma_{d-1}^2, \quad (1.6)$$

where $d\Sigma_{d-1}^2$ is the metric on a unit $(d-1)$ -dimensional hyperbolic plane and Ω is a conformal factor $\Omega = \frac{2R^2}{|R^2 - z^2|} = |1 + \cosh w|$.

In short, $D(A)$ is conformally mapped to $S^1 \times H^{d-1}$. In other words after inverse Wick rotation, we will see that the causal development of the ball enclosed by the entangling surface (SES) is conformally mapped into a hyperbolic cylinder $R \times H^{d-1}$. This mapping, also translates the vacuum of the CFT in the original Minkowski space-time into a thermal bath with temperature $T_0 = \frac{1}{2\pi R}$ in the hyperbolic cylinder.

Note that the curvature scale on the hyperbolic spatial slice, is equal to the radius of the original SES, R . Just like any other operator in CFT, the density matrix in the new space-time $R^1 \times H^{d-1}$ can be achieved by a unitary transformation of the density matrix in the original geometry $R^{1,d-1}$ *i.e.* $\rho_{\text{therm}} = U \rho_A U^{-1}$. More explicitly we may write the density matrix on $D(A)$ as

$$\rho_A = U^{-1} \frac{e^{-H/T_0}}{Z(T_0)} U, \quad Z(T_0) = \text{tr}(e^{-H/T_0}). \quad (1.7)$$

By considering n copies of ρ_A and taking its trace we can compute $\text{tr} \rho_A^n$

$$\text{tr}[\rho_A^n] = \frac{e^{-nH/T_0}}{Z(T_0)^n} = \frac{Z(T_0/n)}{Z(T_0)^n}. \quad (1.8)$$

Now by using the definition of free energy $F(T) = -T \log(Z(T))$ we can write the Rényi entropy as

$$S_n = \frac{1}{1-n} \log \left(\frac{Z(T_0/n)}{Z(T_0)^n} \right) = \frac{n}{(1-n)T_0} \left\{ F(T_0) - F\left(\frac{T_0}{n}\right) \right\}. \quad (1.9)$$

Finally by thermodynamical identity $S = -\partial F/\partial T$, one can rewrite the S_n as

$$S_n = \frac{n}{(n-1)T_0} \int_{T_0/n}^{T_0} S_{\text{therm}}(T) dT. \quad (1.10)$$

Here, S_n is the desired entanglement Rényi entropy between two subsystems A and its complement in the vacuum of CFT and $S_{\text{therm}}(T)$ denotes the thermal entropy of the CFT. Upon taking $n \rightarrow 1$ limit of the above formula, we see that $S_{EE} = \lim_{n \rightarrow 1} S_n = S_{\text{therm}}(T_0)$, which means that the conformal transformation discussed above (and its corresponding unitary transformation) relates the EE of SES to the thermal entropy of the same CFT at temperature T_0 in $R^1 \times H^{d-1}$ space.

This insight might not be particularly useful in the computation of EE for a generic CFT unless using the AdS/CFT correspondence. We can relate the thermal bath in the boundary to a topological black hole in the AdS bulk space whose event horizon has a hyperbolic cross-section [22–27]. According to the AdS/CFT dictionary

$$S_{\text{therm}}(T) \Big|_{\text{CFT in } R^1 \times H^{d-1} \text{ geometry}} = S_{\text{therm}}(T) \Big|_{\text{hyperbolic BH}}. \quad (1.11)$$

The right hand side of this equation is easy to compute by using the Wald’s formula for entropy [28, 29] in any general gravitational theory.

The authors in [30] use this method to find the Rényi entropies of dual CFTs by finding the thermal entropy for black holes in Einstein, Gauss-Bonnet (GB) and quasi-topological gravitational theories. Moreover the authors in [31, 32] expand the aforementioned method to compute ERE for grand canonical ensembles which requires charged black hole and a $U(1)$ gauge field. The computation of charged Rényi entropies in [33, 34] shows that the Rényi entropy inequalities put a new restriction on the allowed values of the coupling constants of the GB gravitational theory.

The Rényi entropies obey the following inequalities [35]

$$\frac{\partial S_n}{\partial n} \leq 0, \quad (1.12a)$$

$$\frac{\partial}{\partial n} \left(\frac{n-1}{n} S_n \right) \geq 0, \quad (1.12b)$$

$$\frac{\partial}{\partial n} ((n-1)S_n) \geq 0, \quad (1.12c)$$

$$\frac{\partial^2}{\partial n^2} ((n-1)S_n) \leq 0. \quad (1.12d)$$

As discussed in [30], while the second and third inequalities are coming from the positivity of black hole thermal entropy the first and last inequalities are correct as long as the black hole has a positive specific heat. For a recent study of these inequalities see [36].

In [37] it was shown that adding a scalar field to the Einstein gravitational action allows a “hairy” black hole solution after a critical temperature and this encourages us to study the Rényi entropies of the dual CFT at this phase transition. It was also shown

that at this critical temperature where the scalar field condenses, the second derivative of Rényi entropy becomes discontinuous. Similar phase transitions occur in the study of holographic superconductors [38] where it might cause a phase transition in the dual boundary CFT. For a review on holographic superconductors see [39].

Inspired by the works in [37] and [34] we are going to add a scalar field to the GB gravity to study the phase transition in presence of new gravitational couplings. We also find new restrictions on the allowed region of the GB coupling constant by studying the Rényi entropy inequalities.

The organization of paper is as follow: In section 2 we introduce Einstein and hairy black holes and compute their physical quantities such as temperature, energy and thermal entropy and discuss about the condensation. We also review related holographic Rényi entropy and its behavior under the phase transition. In section 3 we will add the Gauss-Bonnet terms and investigate the effect of these higher derivative terms to previous results of section 2. In last section we discuss above our results and inequalities in HRE.

2 Phase transition and Rényi entropy

In this section we will review the phase transition between Einstein and hairy black holes in five dimensions which have been already studied in [37] and [40]. We also show the behavior of Rényi entropies under scalar field condensation.

2.1 Einstein black hole

We begin this section by introducing the Einstein-Hilbert action together with a cosmological constant term in a five dimensional space-time

$$I = \frac{1}{16\pi G_N} \int d^5x \sqrt{-g} \left(\mathcal{R} + \frac{12}{L^2} \right). \quad (2.1)$$

To study the entanglement entropy of a spherical region with radius R in a quantum field theory side, which is supposed to exist as a gauge theory on $R^1 \times H^{d-1}$ geometry, we need to start from a Schwarzschild-AdS (Einstein) black hole of radius L and with a hyperbolic spatial boundary. Therefore we start from the following ansatz for metric

$$ds^2 = -N(r)^2 F(r) dt^2 + \frac{dr^2}{F(r)} + r^2 d\Sigma_3^2, \quad (2.2)$$

where $d\Sigma_3^2$ is the metric on a unit hyperboloid in three dimensions

$$d\Sigma_3^2 = du^2 + \sinh^2 u (d\theta^2 + \sin^2 \theta d\phi^2). \quad (2.3)$$

Inserting (2.2) into the equations of motion, we find the following solutions for unknown functions of the metric [40]

$$F(r) = \frac{r^2}{L^2} f(r) - 1, \quad f(r) = 1 + \frac{r_H^2 L^2 - r_H^4}{r^4}, \quad N(r) = N = \frac{L}{R}, \quad (2.4)$$

where r_H is the radius of horizon. In a series of straightforward steps we will compute temperature, energy and thermal entropy of this black hole. By knowing the metric we can find temperature of the black hole by using the following definition

$$T = \frac{N}{4\pi} \left[\frac{d}{dr} F(r) \right]_{r=r_H} = \frac{1}{2\pi R} (2r_H L^{-1} - L r_H^{-1}). \quad (2.5)$$

To compute the black hole energy (mass) in asymptotically AdS space-time, one could use the Astekhar-Das formalism [41]. A quick but equivalent way is to expand g_{00} in the metric [40]

$$g_{00}(r) = -N^2 \left(\frac{r^2}{L^2} - 1 - \frac{m}{r^2} + \dots \right). \quad (2.6)$$

For simplicity we assume $R = L$ (we can get ride of this coefficient by a time rescaling). Therefore the black-hole energy will be

$$E = \frac{3V_\Sigma}{16\pi G_N} m = \frac{3V_\Sigma}{16\pi G_N} (r_H^4 L^{-2} - r_H^2), \quad (2.7)$$

where V_Σ is the regularized volume of the hyperbolic space. Finally to compute the thermal entropy one can use the Wald's formula [28, 29]

$$S_{\text{therm}} = -2\pi \int_{\text{horizon}} d^3x \sqrt{h} \frac{\partial \mathcal{L}}{\partial R_{abcd}} \hat{\varepsilon}_{ab} \hat{\varepsilon}_{cd}. \quad (2.8)$$

In this formula h is the determinant of induced metric on the horizon and $\hat{\varepsilon}_{ab}$ is a binormal composed from the Killing vectors ξ_b and normal vectors to the horizon η_a , *i.e.* $\hat{\varepsilon}_{ab} = \eta_a \xi_b - \eta_b \xi_a$. In the present case this coincides with the Bekenstein-Hawking area formula

$$S_{\text{therm}} = \frac{\mathcal{A}_{\text{horizon}}}{4G_N} = \frac{r_H^3}{4} \frac{V_\Sigma}{G_N}. \quad (2.9)$$

For future proposes it would be useful to introduce a dimensionless parameter $\frac{r_H}{L} \equiv x$, so that the temperature, energy and thermal entropy of the black hole can be written as

$$\tilde{T} = \frac{1}{2\pi} \left(2x - \frac{1}{x} \right), \quad \tilde{E} = \frac{3}{16\pi} x^2 (x^2 - 1), \quad \tilde{S} = \frac{x^3}{4}, \quad (2.10)$$

where we have assumed $R = L = \frac{V_\Sigma L^2}{G_N} = 1$ for simplicity. It is easy to show that the first law of thermodynamics, $d\tilde{E} = \tilde{T} d\tilde{S}$, is satisfied by the above results. Now we can go one step further and find the Rényi entropies where we have introduced in (1.10) by integrating the thermal entropy

$$S_n = \frac{n}{n-1} \int_{\frac{T_0}{n}}^{T_0} S_{\text{therm}} dT = \frac{n}{T_0(n-1)} \int_{x_n}^1 \tilde{S}(x) \frac{d\tilde{T}}{dx} dx = \frac{1}{8} \frac{n}{n-1} (2 - x_n^2 (x_n^2 + 1)), \quad (2.11)$$

where $T(x)|_{x=x_n} = \frac{T_0}{n}$ and T_0 is related to the length scale of the hyperbolic space via $T_0 = \frac{1}{2\pi}$. In order to draw S_n versus n , we should substitute x_n in S_n , which is the real positive root of the following quadratic equation

$$\frac{1}{2\pi} \left(2x_n - \frac{1}{x_n} \right) = \frac{1}{2\pi n} \Rightarrow x_n = \frac{1}{4n} (1 + \sqrt{1 + 8n^2}). \quad (2.12)$$

By doing this we find

$$\tilde{S}_n = \frac{40n^4 - 12n^2 - 1 - (1 + 8n^2)\sqrt{1 + 8n^2}}{256(n-1)n^3}. \quad (2.13)$$

In the limit $n \rightarrow 1$, $\tilde{S}_1 = \frac{1}{4}$ becomes the entanglement entropy and when $n \rightarrow \infty$ the Rényi entropy goes to $\tilde{S}_\infty \rightarrow \frac{5}{32}$ (see figure 1). Moreover one can simply check that all four inequalities in (1.12a)-(1.12d) hold for Rényi entropy of (2.13).

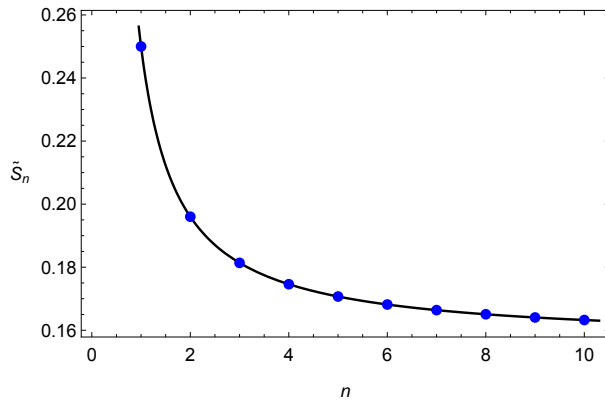


Figure 1: Rényi entropies from hyperbolic black hole solution

2.2 Hairy black hole

In this section we will review the scalar field condensation around a black hole solution in AdS space-time with hyperbolic spatial slicing. We also study the effect of condensation (phase transition) on values of Rényi entropies. To begin, we add a kinetic and a mass term for scalar field to our previous action (2.1)

$$I = \frac{1}{16\pi G_N} \int d^5x \sqrt{-g} \left(\mathcal{R} + \frac{12}{L^2} - \mu^2 \psi^2 - (\nabla\psi)^2 \right). \quad (2.14)$$

To find our desire black hole solution, we choose the following ansatz for metric and scalar field

$$ds^2 = -F(r)e^{2\chi(r)} dt^2 + \frac{dr^2}{F(r)} + r^2 d\Sigma_3^2, \quad \psi = \psi(r). \quad (2.15)$$

The back reaction of the scalar field on the metric will appear through F and χ functions. The equations of motion are

$$\begin{aligned} \psi''(r) + \frac{1}{3L^2 r F(r)} (\psi'(r)[6(2r^2 - L^2) + 3L^2 F(r) - r^2 \mu^2 L^2 \psi(r)^2] - 3r \mu^2 L^2 \psi(r)) &= 0, \\ F'(r) + F(r) \left(\frac{2}{r} + \frac{r}{3} \psi'(r)^2 \right) + \frac{r}{3} \mu^2 \psi(r)^2 + \frac{2}{r} - \frac{4r}{L^2} &= 0, \\ \chi'(r) + \frac{r}{3} \psi'(r)^2 &= 0. \end{aligned} \quad (2.16)$$

To solve this system of coupled nonlinear differential equations numerically, we need to impose boundary conditions on metric and scalar field at horizon ($r = r_H$) and at space-like boundary ($r \rightarrow \infty$) as follows:

- $F(r)$: The definition for location of horizon demands that $F(r_H) = 0$. For asymptotically AdS black holes and at large distances near the infinite boundary, $F(r)$ must behave as $\frac{r^2}{L^2} - 1$.

- $\psi(r)$: To have a hairy black hole we need a regular scalar field at horizon so we suppose that $\psi(r_H) = \mathcal{O}(1)$. As is well known in the dictionary of AdS/CFT, the gravitational bulk theory that we have considered here, must be dual to a conformal field theory that lives at the boundary of AdS space. This CFT contains a scalar operator with conformal dimension Δ , where $\mu^2 L^2 = \Delta(\Delta - 4)$. In order to an asymptotically AdS black hole be unstable against the scalar field condensation, Δ has to be small sufficiently.

We will use the benefits of this instability to study the phase transition due to scalar field condensation. The instability condition requires that the scalar mass to be between two Breitenlohner-Freedman (BF) bounds of AdS_5 and AdS_2 [37, 42, 43]

$$-4 \leq \mu^2 L^2 \leq -1. \quad (2.17)$$

To find the behavior of scalar field at boundary, it will be sufficient to study its equation of motion around the AdS-Schwarzschild background which gives rise to a Klein-Gordon equation. The solution to this equation behaves asymptotically as

$$\psi(r) \approx \frac{A_{(+)}}{r^{\Delta_+}} + \frac{A_{(-)}}{r^{\Delta_-}}, \quad (2.18)$$

where $\Delta_{\pm} = 2 \pm \sqrt{4 + \mu^2 L^2}$, and $A_{(\pm)}$ are the expectation values of the conformal operators with conformal dimensions Δ_{\pm} , *i.e.* $\langle O_{\Delta_{\pm}} \rangle \equiv A_{(\pm)}$. If we assume the Dirichlet boundary condition then we can keep the fastest fall off mode near the boundary and ignore the other one so we choose, $A_{(-)} = 0$.

• $\chi(r)$: By using the third equation of (2.16) and from two boundary conditions for $\psi(r)$, it is easy to obtain the boundary conditions for $\chi(r)$

$$\chi(r \rightarrow \infty) = \mathcal{O}(r^{-2\Delta_+}) + \dots, \quad \chi(r_H) = \mathcal{O}(1). \quad (2.19)$$

In this paper we are going to find numerical solutions for equations of motion by shooting method. To do this it would be easier to change the radial variable from r to z via $z = \frac{r_H}{r}$, which therefore the region $r_H \leq r < \infty$ now converts to $1 \geq z > 0$. Here we also introduce two dimensionless parameters, $m = -\mu^2 L^2$ and $z_0 = \frac{r_H}{L}$. By these changes the equations of motion convert to

$$\begin{aligned} \psi''(z) + \frac{1}{z}\psi'(z)\left(1 + \frac{1}{F(z)}\left[2 - \frac{z_0^2}{z^2}\left(4 + \frac{m}{3}\psi(z)^2\right)\right]\right) + m\frac{\psi(z)}{F(z)}\frac{z_0^2}{z^4} &= 0, \\ F'(z) - F(z)\left(\frac{2}{z} + \frac{z}{3}\psi'(z)^2\right) + \frac{z_0^2}{3z^3}m\psi(z)^2 - \frac{2}{z} + \frac{4z_0^2}{z^3} &= 0, \\ \chi'(z) + \frac{z}{3}\psi'(z)^2 &= 0, \end{aligned} \quad (2.20)$$

and boundary conditions become

$$\begin{aligned} F_B(z \rightarrow 0) &\sim \frac{z_0^2}{z^2} - 1, & F_H(z \rightarrow 1) &= 0, \\ \psi_B(z \rightarrow 0) &\sim C_+ z^{\Delta_+}, & \psi_H(z \rightarrow 1) &= \mathcal{O}(1), \\ \chi_B(z \rightarrow 0) &\sim \mathcal{O}(z^{2\Delta_+}), & \chi_H(z \rightarrow 1) &= \mathcal{O}(1). \end{aligned} \quad (2.21)$$

In shooting method we need to calculate the series expansions of scalar and metric functions around the horizon and boundary. By inserting these series into the equations of motion we can find the coefficients of the expansions. After that we match the series smoothly at some small distance, say ϵ , from one end of the interval $0 < z < 1$. Note that for a given $\psi(z)$ one can find $\chi(z)$ from the last equation of motion in (2.16), simply by an integration.

Since equations of motion are regular at horizon the expansion of functions will be Taylor series near the horizon

$$\psi_H(z) = \sum_{n=0}^{\infty} \psi_{(n)}(z-1)^n, \quad F_H(z) = \sum_{n=0}^{\infty} F_{(n)}(z-1)^n. \quad (2.22)$$

Boundary conditions (2.21) require that $F_{(0)} = 0$. By substituting (2.22) into the equations of motion (2.20) and expanding near $z = 1$, we can find $F_{(n)}$ and $\psi_{(n)}$ as functions of z_0 , m and $\psi_{(0)} \equiv \psi_1$. In the precision region of our computations it would be enough to keep expansions up to $n = 6$. For example the first few terms are

$$\begin{aligned}\psi_H(z) &= \psi_1 + (z-1)\left(\frac{3mz_0^2\psi_1}{z_0^2(12+m\psi_1^2)-6}\right) + \dots, \\ F_H(z) &= (z-1)\left(2-4z_0^2-\frac{m}{3}z_0^2\psi_1^2\right) + \dots.\end{aligned}\tag{2.23}$$

Expansion near the boundary at $z = 0$ is a little bit trickier because equations of motion are irregular at this point. Here we have a power series expansion and the power of the leading term depends on the value of m . We denote this mass dependent parameter by δ

$$\psi_B(z) = C_+ z^{\Delta_+} + \dots = \sum_{i=i_{min}}^{\infty} a_i z^{2+i\delta}, \quad F_B(z) = \frac{z_0^2}{z^2} - 1 + \sum_{j=1}^{\infty} b_j z^{j\delta}.\tag{2.24}$$

Here we expand functions until the resulting algebraic system of equations gives a non-trivial solution. In table 1 we have presented the values of m , Δ_+ , δ and i_{min} where we have used to solve the equations of motion numerically

m	4	$\frac{63}{16}$	$\frac{60}{16}$	$\frac{55}{16}$	3	$\frac{39}{16}$
Δ_+	2	$\frac{9}{4}$	$\frac{10}{4}$	$\frac{11}{4}$	3	$\frac{13}{4}$
δ	1	$\frac{1}{4}$	$\frac{1}{2}$	$\frac{1}{4}$	1	$\frac{1}{4}$
i_{min}	0	-1	-1	-3	-1	-5

Table 1: Numerical values for series expansion near the boundary.

By substituting the above expansions for every mass parameter into the equations of motion we can find the expansion coefficients, a_i and b_j in terms of three parameters C_+ , C_m and z_0 , where C_+ is the coefficient of z^{Δ_+} in $\psi_B(z)$ and C_m is the coefficient of z^2 in $F_B(z)$.

In shooting method, we first read the initial values of the fields and their derivatives near the horizon at $z = 1 - \epsilon$ from the series expansion in (2.23), then we solve the first two differential equations in (2.20) numerically to find the values of the fields near the boundary at $z = \epsilon$. After that, we can compare these values of the fields with those which are coming from the near boundary expansion in (2.24). At the end of the day we will have four equations for four unknown parameters C_+ , C_m , ψ_1 and z_0 to solve. This set of equations has innumerable numerical solutions which can be found and put into the power series expansions of the fields both at the horizon and boundary to compute various physical and thermodynamical quantities.

The first interesting quantity is again the temperature of the hairy black hole

$$T = \frac{e^{\chi(r)}}{4\pi} \left| F'(r) \right|_{r=r_H} = \frac{e^{\chi(z)}}{4\pi z_0} \left| F'(z) \right|_{z=1},\tag{2.25}$$

where $F'(1) = 2 - 4z_0^2 - \frac{m}{3}z_0^2\psi_1^2$ is coming from equation (2.23) and

$$\chi(1) = \int_{z=\epsilon}^{1-\epsilon} \left(-\frac{z}{3}\right) (\psi'(z))^2 dz,\tag{2.26}$$

can be computed numerically by imposing the boundary conditions of (2.21).

The next quantity is the thermal entropy of the hairy black hole

$$S_{\text{therm}} = \frac{r_H^3}{4} \frac{V_\Sigma}{G_N} \rightarrow \tilde{S} = \frac{z_0^3}{4}, \quad (2.27)$$

where we have calculated the entropy again in the unit where $\frac{L^3 V_\Sigma}{G_N} = 1$. To compute the energy of hairy black hole we can use two different ways again. Either we can expand g_{00} as before

$$g_{00}(z)_{z \rightarrow 0} = -F(z)e^{2\chi(z)} \Big|_{z \rightarrow 0} = -\frac{z_0^2}{z^2} + 1 + \tilde{m}z^2 + \dots, \quad (2.28)$$

and pick up the coefficient of $\frac{z^2}{z_0^2}$, therefore the energy becomes

$$E = \frac{3V_\Sigma}{16\pi G_N} \tilde{m}z_0^2 \rightarrow \tilde{E} = \frac{3}{16\pi} \tilde{m}z_0^2, \quad (2.29)$$

or we can use the second law of thermodynamics for black holes ($dE = TdS$) numerically and compute the energy. Both ways have the same result.

As we discussed before, in AdS/CFT dictionary the coefficient of $r^{-\Delta_+}$ gives the expectation value of conformal operator O with conformal dimension Δ_+ , this coefficient is called the condensate. In z coordinates the leading order of $\psi(z) \sim C_+ z^{\Delta_+}$ therefore the value of condensate is $\langle O \rangle = C_+ z_0^{\Delta_+}$. Figure 2 shows the behavior of $\langle O \rangle^{\frac{1}{\Delta_+}}$ in terms of temperature for various possible values of Δ_+ in the interval $2 \leq \Delta_+ \leq 2 + \sqrt{3}$. The condensation happens for each value of Δ_+ at a different critical temperature \tilde{T}_c , which decreases when Δ_+ is increasing.

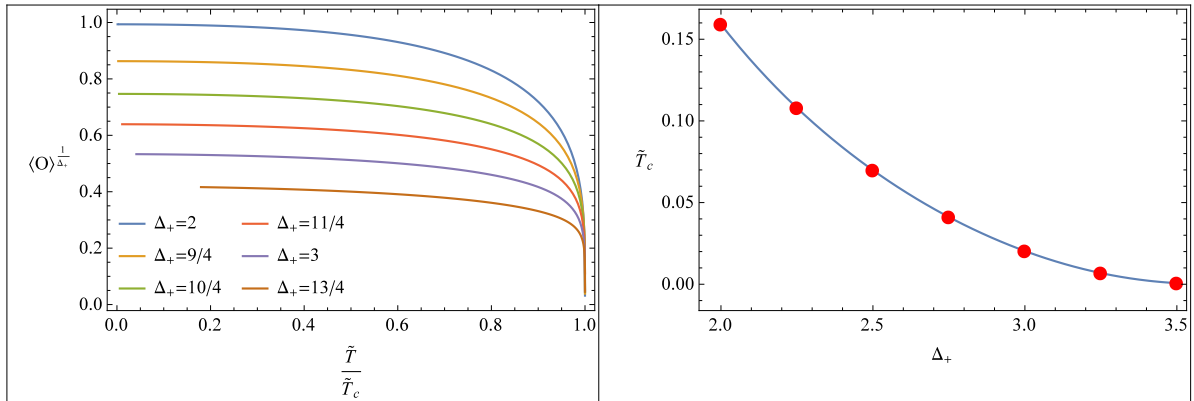


Figure 2: Left: Condensate as a function of temperature (scaled by the corresponding critical temperature) for various values of Δ_+ . The lowest curve belongs to $\Delta_+ = \frac{13}{4}$ and the top curve is for $\Delta_+ = 2$. Right: The critical temperature as a function of Δ_+ .

When the AdS_5 BF bound saturates, *i.e.* $\Delta_+ = 2$ or $m = 4$, the critical temperature T_c reaches to its maximum value at $\tilde{T}_0 = \frac{1}{2\pi} \approx 0.159$. This is the Rindler temperature (temperature of massless black hole).

In following figures we have sketched different behavior of physical quantities in term of energy or temperature.

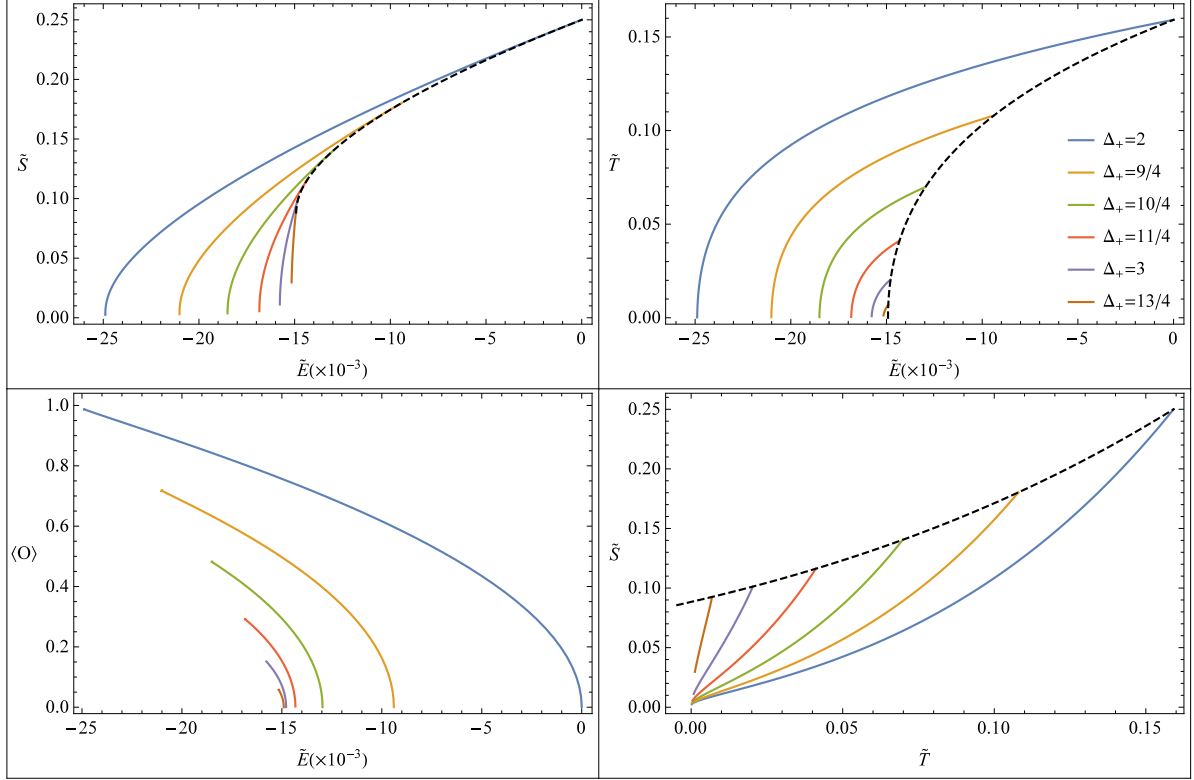


Figure 3: Thermodynamical quantities for various values of Δ_+ . Note that the colors in this figure are matched with the figure 2. The dashed black curve represents Einstein black hole solution and solid curves belong to hairy black holes.

For each diagram in figure 3 the dashed curve represents the Einstein black hole. The $\tilde{S} - \tilde{T}$ diagram shows how condensation happens. As temperature decreases there is a critical temperature for each value of Δ_+ (the point where solid curves meet the dashed one) in which, the Einstein black hole replaces by a hairy black hole. As we see the critical temperature decreases when Δ_+ increases. One can convert the temperature to energy from $\tilde{T} - \tilde{E}$ diagram. The $\tilde{S} - \tilde{E}$ diagram shows that the entropy of a hairy black hole at a specific value of energy is larger than the Einstein black hole therefore the hairy black holes are more favorable (stable) after condensation. The $\langle O \rangle - \tilde{E}$ diagram displays where condensation starts and reaches to its maximum value in terms of energy.

To compute the Rényi entropies from (1.10) according to $\tilde{S} - \tilde{T}$ diagram in figure 3, we should take into account the phase transition from Einstein black hole (EBH) to hairy black hole (HBH) [37]

$$S_n = \frac{n}{T_0(n-1)} \left\{ \int_{T_0/n}^{T_c} S_{\text{therm}}^{\text{HBH}}(T) dT + \int_{T_c}^{T_0} S_{\text{therm}}^{\text{EBH}}(T) dT \right\}. \quad (2.30)$$

The second term above differs from (2.11) only on its lower limit. Here we can define $T(x)|_{x=x_c} = T_c$ in accordance with the definition of x_n . So \tilde{S}_n becomes

$$\begin{aligned} \tilde{S}_n &= \frac{n}{\tilde{T}_0(n-1)} \left\{ \int_{\tilde{T}_0/n}^{\tilde{T}_c} S_{\text{therm}}^{\text{HBH}}(T) dT + \int_{x_c}^1 \tilde{S}^{\text{EBH}}(x) \frac{d\tilde{T}}{dx} dx \right\} \\ &= \frac{2\pi n}{n-1} \int_{\tilde{T}_0/n}^{\tilde{T}_c} S_{\text{therm}}^{\text{HBH}}(T) dT + \frac{n}{8(n-1)} [2 - x_c^2(x_c^2 + 1)], \end{aligned} \quad (2.31)$$

where x_c is the real positive root of $\frac{1}{2\pi} \left(2x_c - \frac{1}{x_c} \right) = \tilde{T}_c$ or $x_c = \frac{\pi \tilde{T}_c}{2} \left(1 + \sqrt{1 + \frac{2}{(\pi \tilde{T}_c)^2}} \right)$. By some numerical computation we can draw \tilde{S}_n in terms of n , see figure 4.

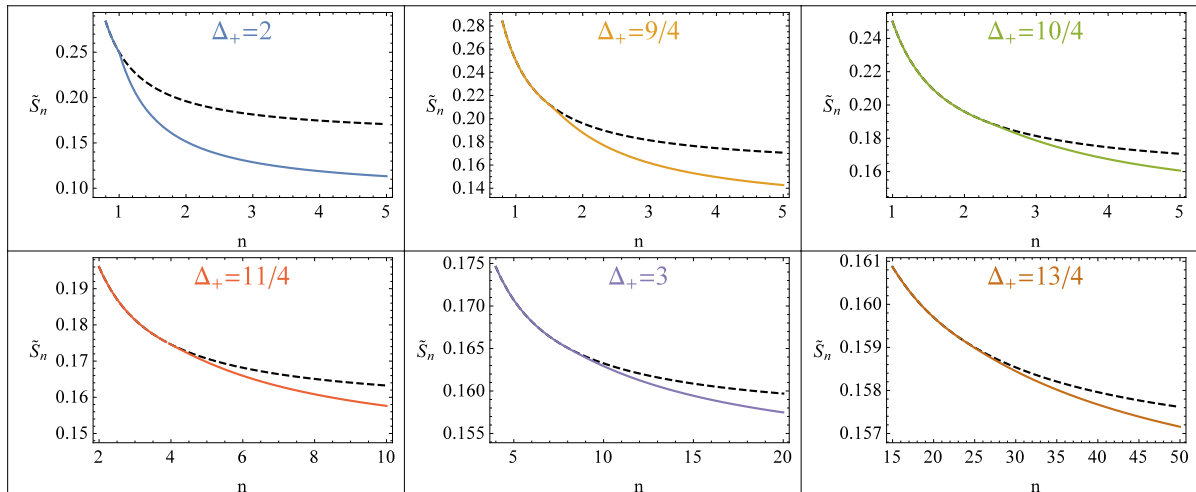


Figure 4: Each diagram shows the behavior of Rényi entropies for EBH (dashed curve) and HBH for different values of Δ_+ . Two curves meet each other at n_c .

As we observe from figure 4, one can define a critical number $n_c = \frac{\tilde{T}}{T_c}$, where the curve of HBH approaches that of EBH. At this point the second derivative of \tilde{S}_n suddenly changes. This discontinuity of the second derivative of \tilde{S}_n with respect to n confirms that the condensation of the scalar field is a second order phase transition. Moreover the value of n_c increases by increasing of Δ_+ as we depicted in figure 5. Here all four inequalities (1.12a)-(1.12d) hold again.

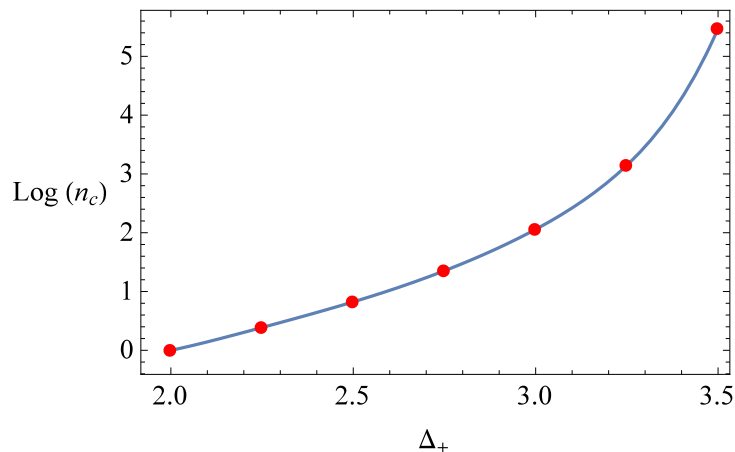


Figure 5: Logarithm of the critical Rényi parameter as a function of Δ_+ .

3 Entanglement Rényi entropy from Gauss-Bonnet gravity

In this section, we are going to explore the effect of higher curvature bulk theories of gravity on condensation and holographic Rényi entropy. We consider the Gauss-Bonnet (GB) gravity in five dimensions where equations of motion are of second order in derivatives and the numerical method of previous section works here as well without any further boundary condition.

3.1 Modified Einstein Gauss-Bonnet black hole

Similar to previous section we start from a pure gravitational action in five dimensions

$$I = \frac{1}{16\pi G_N} \int d^5x \sqrt{-g} \left\{ \mathcal{R} + \frac{12}{L^2} + \frac{\lambda L^2}{2} \left(\mathcal{R}_{abcd} \mathcal{R}^{abcd} - 4\mathcal{R}_{ab} \mathcal{R}^{ab} + \mathcal{R}^2 \right) \right\}, \quad (3.1)$$

where λ is a free dimensionless coupling. To find asymptotically AdS black hole solutions with hyperbolic horizon, we use again the ansatz in equation (2.2) and insert it into the equations of motion. We will find

$$\left(1 - \frac{2\lambda L^2}{r^2} (1 + F(r)) \right) F'(r) + \frac{2}{r} (1 + F(r)) - \frac{4r}{L^2} = 0, \quad \frac{dN(r)}{dr} = 0, \quad (3.2)$$

with the following Einstein Gauss-Bonnet (EGB) black hole solution

$$F(r) = \frac{r^2}{L^2} f(r) - 1 = \frac{r^2}{L^2} \left(\frac{1}{2\lambda} \left[1 - \sqrt{1 - 4\lambda \left(1 - \frac{C}{r^4} \right)} \right] \right) - 1, \quad (3.3)$$

where the constant of integration is fixed in terms of the horizon radius by demanding that $F(r)$ vanishes at horizon, *i.e.* $C = r_H^4 - r_H^2 L^2 + \lambda L^4$. By comparing (3.3) with equation (2.4) we can fix the constant value of $N(r) = N$. Since asymptotically $f(r) \rightarrow f_\infty = \frac{1}{2\lambda} (1 - \sqrt{1 - 4\lambda})$ we can choose

$$N = \frac{L\sqrt{2\lambda}}{R\sqrt{(1 - \sqrt{1 - 4\lambda})}} \equiv \frac{L_{\text{eff}}}{R}, \quad (3.4)$$

where L_{eff} is an effective asymptotic AdS scale. Note that asymptotically $F(r) \rightarrow \frac{r^2}{L_{\text{eff}}^2} - 1$.

By avoiding imaginary AdS scale or naked singularity the Gauss-Bonnet coupling λ is limited to $\lambda \leq 1/4$. On the other hand the unitarity of the boundary theory dual to the Gauss-Bonnet gravity in this background demands that $-\frac{7}{36} \leq \lambda \leq \frac{9}{100}$, for example see [44]. Therefore we will restrict our numerical computations to this unitary interval from now on.

Now we follow analogous steps similar to the section two, to calculate the thermodynamical quantities and then compute the holographic Rényi entropy. The black hole temperature is given by

$$T = \frac{N}{4\pi} \frac{\partial F(r)}{\partial r} \Big|_{r=r_H} = \frac{L_{\text{eff}}}{4\pi R L^2} \frac{2r_H(2r_H^2 - L^2)}{r_H^2 - 2\lambda L^2}. \quad (3.5)$$

By introducing $X = \frac{r_H}{L_{\text{eff}}}$ and $T_0 = \frac{1}{2\pi R}$, the temperature can be expressed as [30]

$$T = \frac{T_0 X (2X^2 - f_\infty)}{f_\infty (X^2 - 2\lambda f_\infty)} \equiv 2\pi T_0 \tilde{T}. \quad (3.6)$$

To compute the black hole energy we use again the procedure discussed in section two. By expanding the metric near the boundary and assuming $R = L_{\text{eff}}$ we have

$$g_{00}(r) \Big|_{r \rightarrow \infty} = - \left\{ \frac{r^2}{L_{\text{eff}}^2} - 1 - \frac{C}{r^2 L^2 \sqrt{1 - 4\lambda}} + \dots \right\}. \quad (3.7)$$

Therefore the black hole energy becomes

$$\begin{aligned}
E &= \frac{3V_\Sigma}{16\pi G_N} \left(\frac{r_H^4 - r_H^2 L^2 + \lambda L^4}{L^2 \sqrt{1 - 4\lambda}} \right) \\
&= \frac{3V_\Sigma L^2}{16\pi G_N} \frac{X^4 - f_\infty X^2 + \lambda f_\infty^2}{f_\infty^2 \sqrt{1 - 4\lambda}} \equiv \left(\frac{V_\Sigma L^2}{G_N} \right) \tilde{E},
\end{aligned} \tag{3.8}$$

where \tilde{E} is the dimensionless energy of EGB black hole. As was mentioned in section two, in higher derivative gravitational theories we must use the Wald's formula (2.8) to compute the thermal entropy. After a little computation we find

$$\frac{\partial \mathcal{L}_{GB}}{\partial R_{abcd}} \hat{\varepsilon}_{ab} \hat{\varepsilon}_{cd} = \frac{1}{16\pi G_N} \left\{ \frac{12\lambda L^2}{r^2} [1 + F(r)] - 2 \right\}, \tag{3.9}$$

from which we can compute the thermal entropy as

$$\begin{aligned}
S_{\text{therm}} &= \frac{V_\Sigma}{4G_N} r_H^3 \left(1 - \frac{6\lambda L^2}{r_H^3} \right) \\
&= \frac{V_\Sigma L^3}{G_N} \frac{X^3 - 6\lambda X f_\infty}{4f_\infty^{3/2}} \equiv \left(\frac{V_\Sigma L^3}{G_N} \right) \tilde{S}_{\text{therm}}.
\end{aligned} \tag{3.10}$$

By knowing the thermal entropy now we can compute the holographic Rényi entropy. Using the equation (2.11) and defining $T(X)|_{X=X_n} = \frac{T_0}{n}$, we find [30]

$$\begin{aligned}
S_n &= \frac{n}{T_0(n-1)} \int_{X_n}^1 S(X) \frac{dT}{dX} = \frac{n}{T_0(n-1)} \int_{X_n}^1 \left(\frac{L^3 V_\Sigma}{G_N} \tilde{S}_{\text{therm}} \right) \left(\frac{1}{R} \frac{d\tilde{T}}{dX} \right) dX \\
&= \frac{n}{n-1} \frac{L^3 V_\Sigma}{G_N} \frac{1}{8f_\infty^{5/2}} \left(9(1 - X_n^4) - 3f_\infty(1 - X_n^2) + \frac{4(f_\infty - 2)}{1 - 2\lambda f_\infty} - \frac{4X_n^4(f_\infty - 2X_n^2)}{X_n^2 - 2\lambda f_\infty} \right).
\end{aligned} \tag{3.11}$$

Note that X_n in above equation is the real positive root of the following cubic equation

$$2nX_n^3 - f_\infty X_n^2 - nf_\infty X_n + 2\lambda f_\infty^2 = 0. \tag{3.12}$$

In [33] and [34] the authors show that in Gauss-Bonnet gravity there is a new bound on coupling λ when we demand the positivity of thermal entropy. In five dimensions this is $-\frac{7}{36} \leq \lambda \leq \frac{1}{12}$. We will discuss this in the next section.

3.2 Modified hairy black hole

In section two we reviewed the condensation of scalar field around a five dimensional asymptotically AdS black hole with hyperbolic horizon in Einstein gravity. In this section we are going to study the effect of higher derivative terms on scalar condensation, by considering the Gauss-Bonnet gravity. We will first prove the existence of a non-trivial scalar solution below the critical temperature and then compare the thermodynamical properties and holographic Rényi entropy with those hairy black hole of the Einstein gravity, in various values of the scalar mass μ and coupling λ . We start from the following action where a real scalar field is coupled to gravity

$$I = \frac{1}{16\pi G_N} \int d^5x \sqrt{-g} \left\{ \mathcal{R} + \frac{12}{L^2} + \frac{\lambda L^2}{2} \left(\mathcal{R}_{abcd} \mathcal{R}^{abcd} - 4\mathcal{R}_{ab} \mathcal{R}^{ab} + \mathcal{R}^2 \right) - \mu^2 \psi^2 - (\nabla \psi)^2 \right\}. \tag{3.13}$$

The metric and scalar field ansatz that we will use for Gauss-Bonnet gravity are the same as those in equation (2.15). The equations of motion for action (3.13) are

$$\begin{aligned}
&\psi''(r) + \frac{1}{3L^2 r F(r) [1 - V(\lambda, r)]} \left\{ \psi'(r) [6(2r^2 - L^2) + 3L^2 - \mu^2 L^2 r^2 \psi(r)^2 \right. \\
&\quad \left. - 9L^2 F(r) V(\lambda, r)] - 3\mu^2 L^2 r \psi(r) [1 - V(\lambda, r)] \right\} = 0, \\
&F'(r) + \frac{1}{[1 - V(\lambda, r)]} \left\{ F(r) \left[\frac{2}{r} + \frac{r}{3} \psi'(r)^2 \right] + \frac{r}{3} \mu^2 \psi(r)^2 + \frac{2}{r} - \frac{4r}{L^2} \right\} = 0, \\
&\chi'(r) - \frac{r}{3[1 - V(\lambda, r)]} \psi'(r)^2 = 0,
\end{aligned} \tag{3.14}$$

where we have defined $V(\lambda, r) = \frac{2\lambda L^2}{r^2} (1 + F(r))$. Since in Gauss-Bonnet gravity the equations of motion remain at second order of derivatives therefore the number of boundary conditions are the same as before. Similar to previous section, we need to know the behavior of every unknown function at the horizon $r = r_H$ and near the boundary as $r \rightarrow \infty$.

As always, the definition of the location of horizon $F(r = r_H) = 0$ gives the first boundary condition on $F(r)$. On the other hand, as we mentioned before, the asymptotic behavior of this function is given by

$$F(r \rightarrow \infty) \sim \frac{r^2}{L_{\text{eff}}^2} - 1, \quad L_{\text{eff}}^2 = \frac{2\lambda L^2}{1 - \sqrt{1 - 4\lambda}} \tag{3.15}$$

We also demand that the scalar field to be a regular function at horizon so $\psi(r_H) = \mathcal{O}(1)$. If we consider the scalar field as a quantum field living in the curved space-times outside black hole horizon, even in the presence of Gauss-Bonnet terms, it should satisfy the Klein-Gordon equation. The solution of this equation decays at infinity as $\psi(r) \sim \frac{A_{(+)}}{r^{\Delta_+}} + \frac{A_{(-)}}{r^{\Delta_-}}$.

As we discussed before, $A_{(\pm)}$ are the expectation values of conformal operators with Δ_{\pm} conformal dimensions. To find a relation for Δ one needs to substitute $F(r) = \frac{r^2}{L_{\text{eff}}^2} - 1$ and $\psi(r) = Ar^{-\Delta}$ into the equation of motion for scalar field (first equation in (3.14)) in the limit of $r \rightarrow \infty$. In this regard we will find the following values for conformal dimension

$$\Delta_{\pm} = 2 + \sqrt{4 + \mu^2 L_{\text{eff}}^2}. \tag{3.16}$$

In what follows we again assume the Dirichlet boundary conditions, $A_{(-)} = 0$, therefore we expect $\psi(r \rightarrow \infty) \sim \frac{A}{r^{\Delta_+}}$ asymptotically.

It is also easy to derive the boundary conditions on $\chi(r)$ just by looking at the last equation of motion in (3.14)

$$\chi(r_H) = \mathcal{O}(1), \quad \chi(r \rightarrow \infty) = \mathcal{O}(r^{-2\Delta_+}) + \dots \tag{3.17}$$

We can use the advantage of working with the dimensionless parameters which is desirable in numerical methods. To do this we change the radial coordinate from r to z via $z = \frac{r_H}{r}$ and introduce a dimensionless mass parameter $m = -\mu^2 L^2$. We also use the scaling symmetry of the equations of motion to define $z_0 = \frac{r_H}{L_{\text{eff}}}$. Then the equations of motion

will be the followings

$$\begin{aligned}
\psi''(z) + \frac{\psi'(z)}{z[1-V(\lambda, z)]} \left\{ 1 + \frac{1}{F(z)} \left[2 - \frac{z_0^2}{f_\infty z^2} (4 + \frac{m}{3} \psi(z)^2) \right] + V(\lambda, z) \right\} + \frac{\psi(z)}{F(z)} \frac{m z_0^2}{f_\infty z^4} &= 0, \\
F'(z) + \frac{1}{z[1-V(\lambda, z)]} \left\{ -F(z) \left[2 + \frac{z^2}{3} \psi'(z)^2 \right] + \frac{z_0^2 m}{3 z^2 f_\infty} \psi(z)^2 - 2 + \frac{4 z_0^2}{z^2 f_\infty} \right\} &= 0, \\
\chi'(z) + \frac{z}{3[1-V(\lambda, z)]} \psi'(z)^2 &= 0,
\end{aligned} \tag{3.18}$$

where

$$V(\lambda, z) = \frac{2\lambda z^2 f_\infty}{z_0^2} (1 + F(z)), \quad \frac{L^2}{L_{\text{eff}}^2} = f_\infty = \frac{1 - \sqrt{1 - 4\lambda}}{2\lambda}. \tag{3.19}$$

The boundary condition also can be written as

$$\begin{aligned}
F_B(z \rightarrow 0) &\sim \frac{z_0^2}{z^2} - 1, & F_H(z \rightarrow 1) &= 0, \\
\psi_B(z \rightarrow 0) &\sim C_+ z^{\Delta_+}, & \psi_H(z \rightarrow 1) &= \mathcal{O}(1), \\
\chi_B(z \rightarrow 0) &\sim \mathcal{O}(z^{2\Delta_+}), & \chi_H(z \rightarrow 1) &= \mathcal{O}(1).
\end{aligned} \tag{3.20}$$

These boundary conditions are identical to those in (2.21).

As we discussed in section two, in order to find a numerical solution for equations of motion we need to compute the expansion of metric and scalar functions near the horizon and boundary. Once again we substitute the near horizon expansion (2.22) into the first two equations of motion in (3.18) and expand near $z = 1$. We find

$$\begin{aligned}
\psi_H(z) &= \psi_1 + (z - 1) \left[\frac{3m\psi_1(z_0^2 - 2\lambda f_\infty)}{z_0^2(12 + m\psi_1^2) - 6f_\infty} \right] + \dots \\
F_H(z) &= (z - 1) \frac{z_0^2}{3f_\infty} \left[\frac{6f_\infty - z_0^2(12 + m\psi_1^2)}{z_0^2 - 2\lambda f_\infty} \right] + \dots
\end{aligned} \tag{3.21}$$

Similarly we use the near boundary expansion at $z = 0$ in equation (2.24) but here we note that the leading order is given by the value of Δ_+ in equation (3.16) or $\Delta_+ = 2 + \sqrt{4 - \frac{m}{f_\infty}}$ equivalently. Here we will have a two-parameter family of solutions which are controlled by the values of m and f_∞ or equivalently by μ and λ . In our numerical method it would be simpler to fix the value of Δ_+ firstly and then choose some appropriate values for dimensionless mass and coupling.

As we discussed before, in shooting method we first read the initial values of the fields and their derivatives near the horizon and then solve the equations of motion numerically, to find the values of the fields near the boundary. By comparing with the values of the near boundary expansion we will find four equations for four unknown parameters C_+ , C_m , ψ_1 and z_0 . The values of these parameters can be used to compute the various physical and thermodynamical quantities of our problem.

The temperature of modified hairy black hole is given by $\tilde{T} = \frac{e\chi(z)}{4\pi z_0} |F'(z)| \Big|_{z=1}$, where from (3.21) and (3.18) we have

$$\begin{aligned}
F'(1) &= \frac{z_0^2}{3f_\infty} \left(\frac{6f_\infty - z_0^2(12 + m\psi_1^2)}{z_0^2 - 2\lambda f_\infty} \right), \\
\chi(1) &= \int_{z=\epsilon}^{1-\epsilon} \frac{-z}{3[1-V(\lambda, z)]} \psi'(z)^2 dz.
\end{aligned} \tag{3.22}$$

The next physical quantity is the thermal entropy which we have calculated it before for EGB black hole from the Wald's entropy formula in (3.10). For modified hairy black hole we can use again this equation just by replacing $r_H \rightarrow z_0 L_{\text{eff}}$. Hence

$$S_{\text{therm}} = \frac{V_{\Sigma} L^3}{G_N} \frac{z_0^3}{4f_{\infty}^{3/2}} \left(1 - \frac{6\lambda f_{\infty}}{z_0^2}\right) \equiv \left(\frac{V_{\Sigma} L^3}{G_N}\right) \tilde{S}. \quad (3.23)$$

The computation of energy is straightforward and we can use the same formula that we found in equations (2.28) and (2.29)

$$E = \frac{3V_{\Sigma}}{16\pi G_N} \tilde{m} z_0^2 L_{\text{eff}}^2 \equiv \frac{V_{\Sigma} L^2}{G_N} \tilde{E}. \quad (3.24)$$

Since we are interested in thermal phase transition we need to find the condensate or $\langle O \rangle = C_+ \left(\frac{z_0}{\sqrt{f_{\infty}}}\right)^{\Delta_+}$. By plotting the condensate versus temperature (see figure 6), we observe that the scalar field condensates at every value of λ within the allowed interval $-\frac{7}{36} \leq \lambda \leq \frac{9}{100}$. As we see in figure 6 for a fixed value of $\Delta_+ = 2$ the critical temperature decreases when the Gauss-Bonnet coupling is increasing.

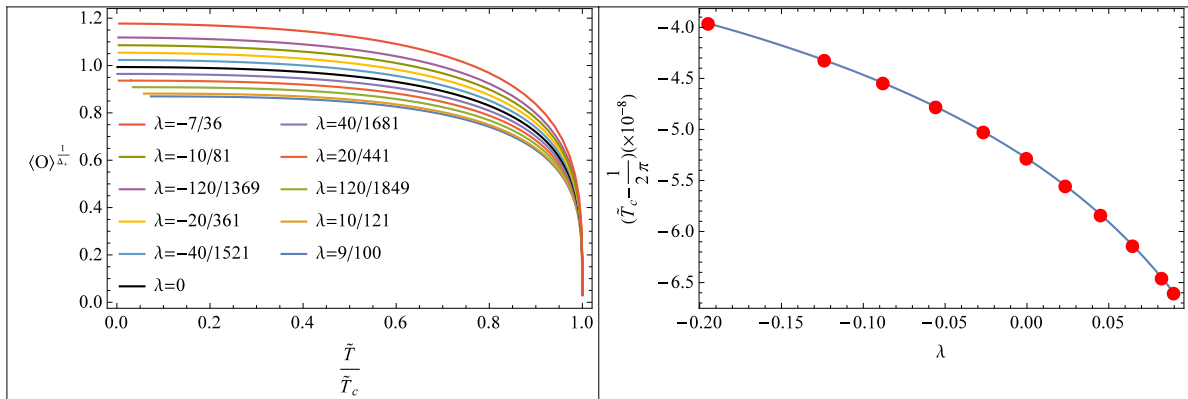


Figure 6: Left: The condensate as a function of temperature (scaled by the corresponding critical temperature) for various values of λ when $\Delta_+ = 2$. The lowest curve is for $\lambda = \frac{9}{100}$ and the top one belongs to $\lambda = -\frac{7}{36}$. Right: Critical temperature as a function of λ .

To see the relation between different thermodynamical quantities and moreover to follow how condensation happens in this theory we have depicted the graphs in figure 7.

The behavior of different quantities are the same as before. We can see this by comparing the curves of $\lambda \neq 0$ with the $\lambda = 0$ (black curve) in each graph. For every value of coupling there is a critical temperature where a phase transition from EGB black hole to modified hairy black hole happens.

But there is an important point here which can be easily seen in $\tilde{S} - \tilde{E}$ or $\tilde{S} - \tilde{T}$ diagrams. For positive values of coupling λ there is a temperature or energy below the critical point where the value of entropy becomes negative. The value of these temperatures T_v , is depicted in figure 8. The same behavior happens for EGB thermal entropy in a narrow region of couplings $\frac{1}{12} < \lambda < \frac{9}{100}$, this has been already reported in [33] and [34].

Finally the Rényi entropies should be computed using the EGB temperature in (3.6). By considering the dimensionless temperature, \tilde{X}_c will be the real positive root of the

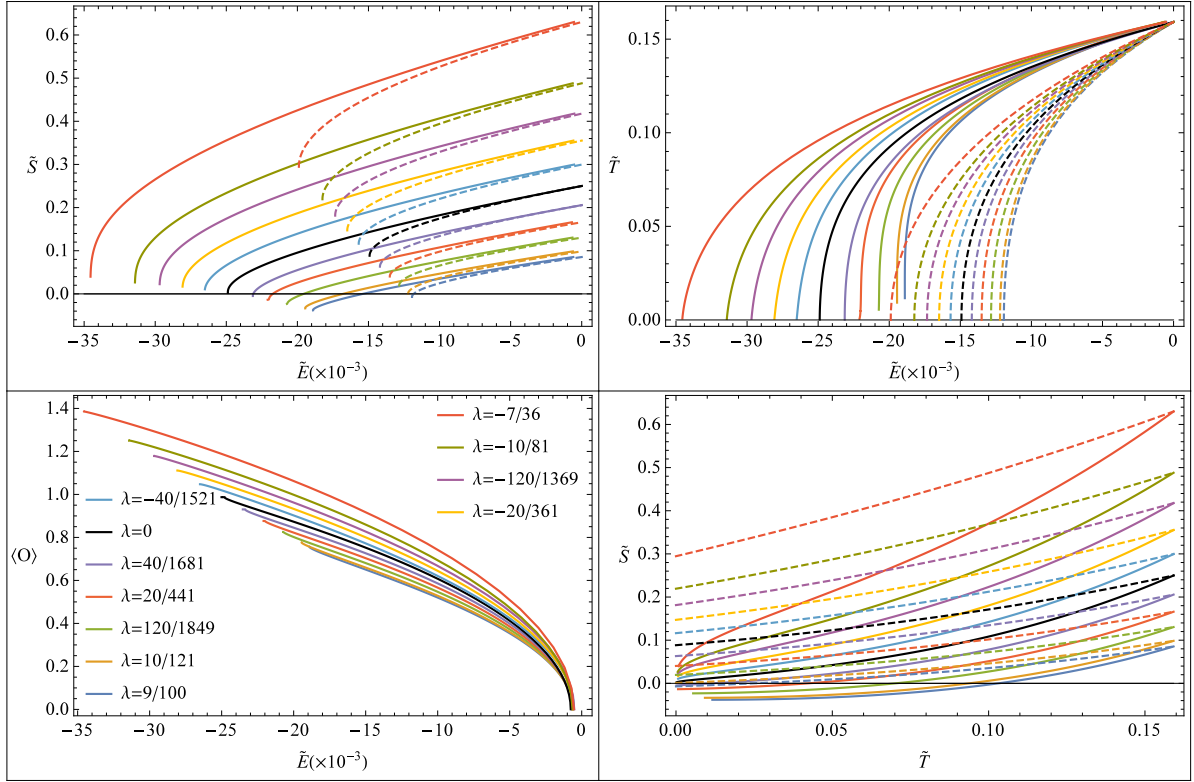


Figure 7: Graphs for thermodynamical quantities in various values of λ when $\Delta_+ = 2$. The colors in this graphs are matched with the figure 6. In each graph a horizontal black line is sketched to guide the zero temperature and zero thermal entropy. The dashed curves represent EGB black hole, while the solid ones represent modified hairy black holes.

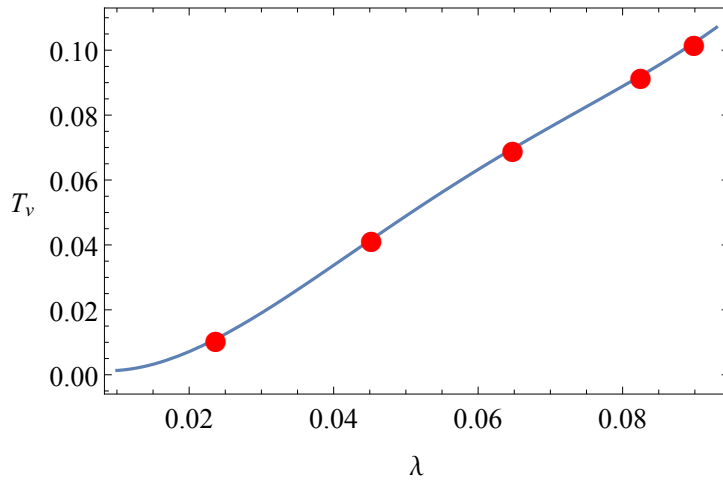


Figure 8: For each positive value of λ there is a temperature T_v , where the thermal entropy becomes negative.

following equation

$$\tilde{X}_c^3 - \tilde{X}_c^2(\pi\tilde{T}_c f_\infty) - \tilde{X}_c\left(\frac{f_\infty}{2}\right) + 2\pi\lambda\tilde{T}_c f_\infty^2 = 0. \quad (3.25)$$

Then according to (3.11), the dimensionless entanglement Rényi entropies become

$$\begin{aligned} \tilde{S}_n = & \frac{2\pi n}{n-1} \int_{\tilde{T}_0/n}^{\tilde{T}_c} \tilde{S}_{\text{thermal}}^{\text{HBBH}}(\tilde{T}) d\tilde{T} + \left(\frac{n}{n-1}\right) \left(\frac{1}{8f_\infty^{5/2}}\right) \left\{ 9(1 - \tilde{X}_c^4) - 3f_\infty(1 - \tilde{X}_c^2) \right. \\ & \left. + \frac{4(f_\infty - 2)}{1 - 2\lambda f_\infty} - \frac{4\tilde{X}_c^4(f_\infty - 2\tilde{X}_c^2)}{\tilde{X}_c^2 - 2\lambda f_\infty} \right\}, \end{aligned} \quad (3.26)$$

where $\tilde{T}_0 = \frac{1}{2\pi}$. Once again the first term of this expression should be computed numerically. Since $\tilde{T}_c \geq \frac{\tilde{T}_0}{n}$ we can define a critical value, $n_c = \frac{\tilde{T}_0}{\tilde{T}_c}$, where the Rényi entropy corresponding to the modified hairy black hole approaches that of the EGB black hole, see figure 9.

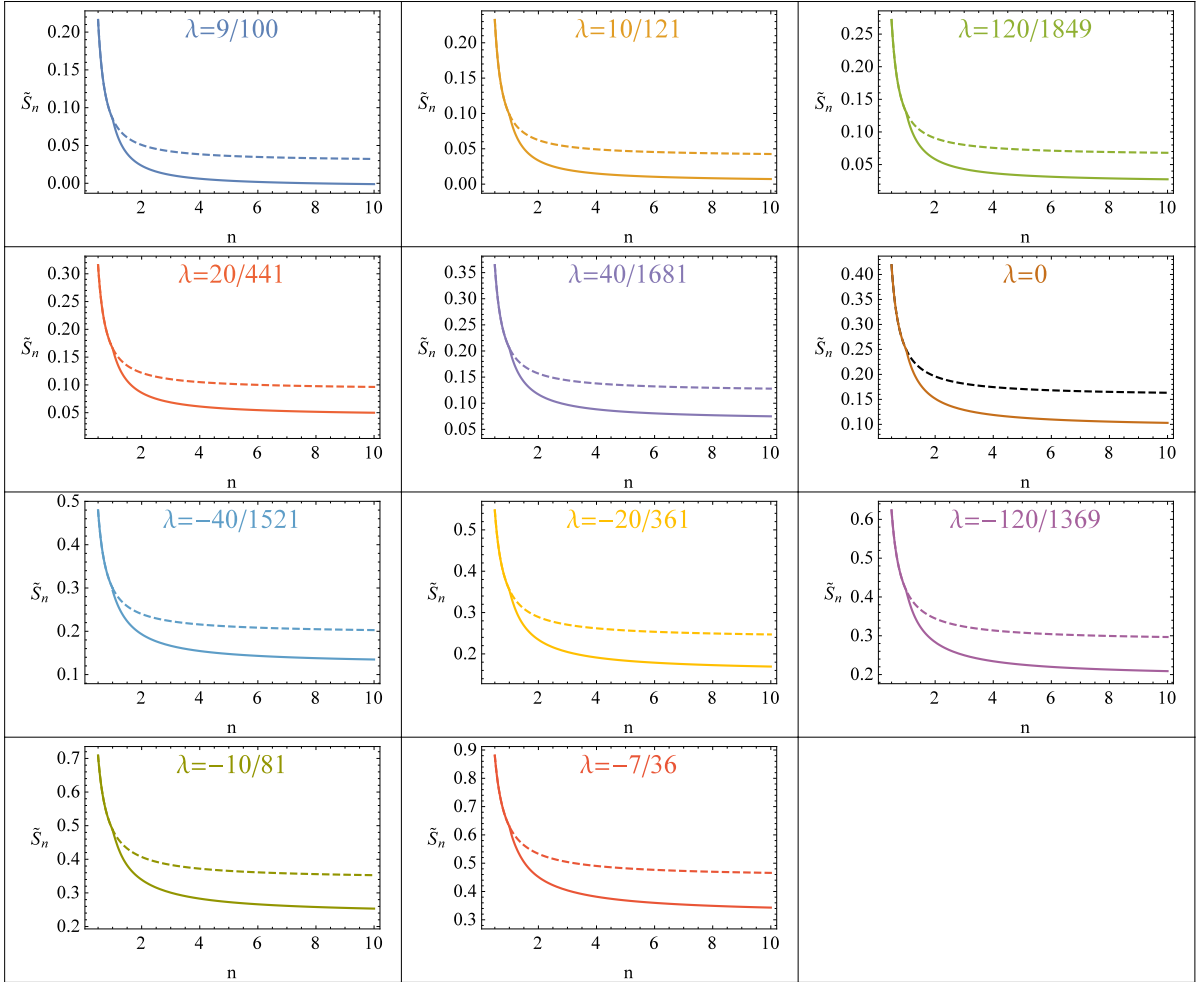


Figure 9: In each diagram there is a critical point where the ERE of modified hairy black hole (solid curve) approaches that of the EGB black hole (dashed curve).

These diagrams show that in the presence of Gauss-Bonnet terms the condensation of the scalar field is again a second order phase transition.

To see the behavior of n_c under the change in coupling λ we have sketched figure 10 (left). As we see this critical value increases when moving from negative values of coupling to positive values.

By computing the Rényi entropy inequalities (1.12a)-(1.12d) we have sketched the corresponding diagrams in terms of n , see figure 11. As we observe the inequalities (1.12a) and (1.12d) hold here but inequality (1.12b) is violated for positive values of coupling λ . This is completely consistent with the fact that for positive values of coupling there is a temperature where the thermal entropy becomes negative. We expect that the same should be happened for the third inequality (1.12c), but as we see this is not true and third inequality still holds. These results have been discussed in the last section of paper.

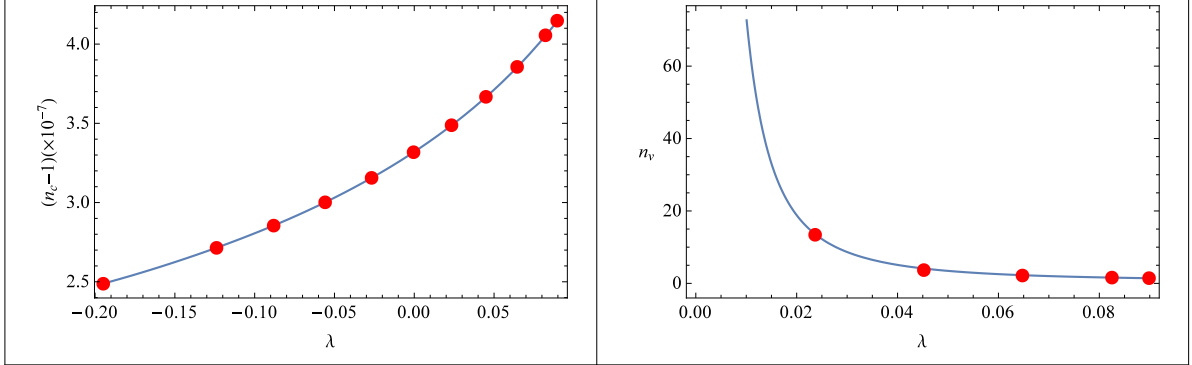


Figure 10: Left: When the scalar mass is $\Delta_+ = 2$, the critical Rényi parameters are extremely close to one. So we have sketched $n_c - 1$ as a function of λ . Right: n_v shows the value of n where the second inequality governing EREs is violated, as a function of λ for all positive values of GB coupling constant.

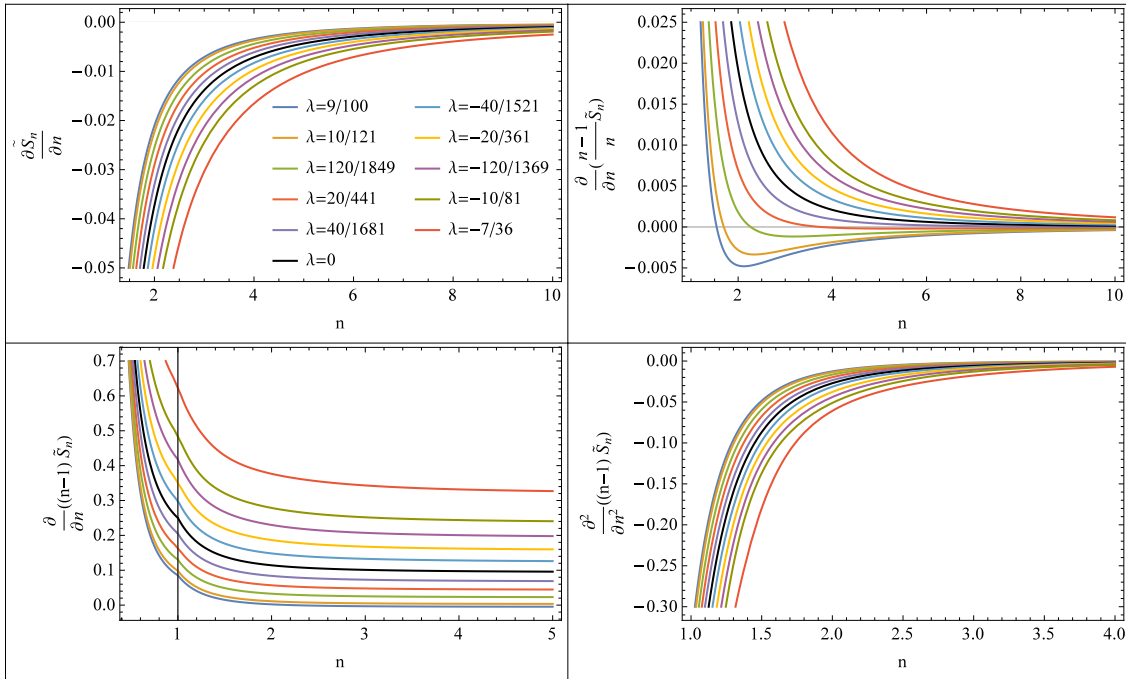


Figure 11: Inequalities of Rényi entropies. The left bottom diagram shows that the phase transition is a second order one.

By a numerical study one can find a violation Rényi parameter, n_v , where the second inequality governing EREs is violated, see the right diagram in figure 10.

3.2.1 Results for $\Delta_+ > 2$

To complete our study of relation between phase transition and Rényi entropies in Gauss-Bonnet gravity we have drawn figure 12 for other values of $\Delta_+ > 2$. In this figure we have presented the critical temperature \tilde{T}_c , critical Rényi parameter n_c and violation Rényi parameter n_v at each value of Gauss-Bonnet coupling λ . The behavior of these parameters are similar to the case of $\Delta_+ = 2$ but is more pronounced as Δ_+ increases.

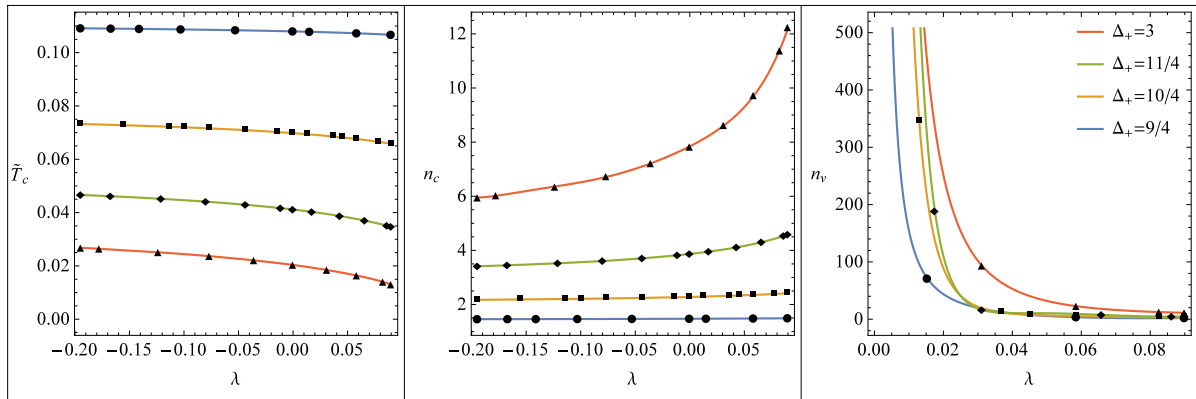


Figure 12: From left to right, the critical temperature, critical Rényi parameter and violation Rényi parameter in terms of GB coupling

4 Discussion

In section 2 of this paper we have reviewed the phase transition from the Einstein black hole to a hairy black hole due to the condensation of a scalar field. Both solutions exist in a five dimensional space-time and have a hyperbolic spatial boundary. The numerical results of condensate in terms of temperature is sketched in figure 2 (left diagram). We have also found the critical temperatures for this phase transition within the unitary bound $2 \leq \Delta_+ \leq 2 + \sqrt{3}$, see figure 2 (right diagram). These diagrams show that by increasing the value of conformal dimension of scalar field the critical temperature of phase transition is dropping. Moreover the value of condensate decreases too.

One can explain this condensation in terms of energy by finding the relation between energy of black holes and their temperatures, $\tilde{T} - \tilde{E}$ diagram in figure 3. The $\tilde{S} - \tilde{E}$ diagram shows that the entropy of a hairy black hole at a specific value of energy is larger than the Einstein black hole so the hairy black hole is more stable than the Einstein black hole after condensation. The $\langle O \rangle - \tilde{E}$ displays that the phase transition happens when the energy decreases.

As reviewed in introduction by knowing the thermal entropy one can compute the entanglement Rényi entropies S_n for a spherical region in the dual gauge theory. The results for these entropies are given in $\tilde{S}_n - n$ diagrams of figure 4. They show the existence of a critical n_c where a discontinuity happens for second derivative of S_n . This suggests that the condensation is a second order phase transition.

In section 3 we have extended the study of phase transition in section 2 by adding Gauss-Bonnet terms to the action. We have modified black hole solutions before and

after the condensation which now depend on the GB coupling λ in the allowed region $-\frac{7}{36} \leq \lambda \leq \frac{9}{100}$. The effect of adding this coupling on condensation is presented in figures 6 and 7. Here we have two important parameters, the conformal dimension of scalar field Δ_+ and coupling λ . We have presented the results for $\Delta_+ = 2$ completely and for $\Delta_+ > 2$ briefly in this paper.

We show that by going from positive values of coupling to negative ones the value of condensate and the critical temperature are increasing, see figure 6. By looking at diagrams $\tilde{S} - \tilde{E}$ or $\tilde{S} - \tilde{T}$ in figure 7 we observe a new behavior for $\lambda > 0$. For positive values of coupling λ there is a temperature or energy below the critical point where the value of entropy becomes negative. The value of these temperatures T_v , is depicted in figure 8.

The entanglement Rényi entropy is calculated in equation (3.26) and for various values of coupling are depicted in figure 9. As we see, a second order phase transition is happening again. The critical points n_c , where the ERE of hairy black holes meet the ERE of the EGB black holes, have been drawn in the left diagram of figure 10.

One important subject in study of entanglement Rényi entropy is the existence of inequalities. We have checked some of these inequalities, (1.12a)-(1.12d) and the reader can see the results of our numerical computation in figure 11. Let us explain our results according to the equation (3.26). To do this, we write the equation (3.26) in a little simpler form

$$\tilde{S}_n = \frac{2\pi n}{n-1} \int_{\tilde{T}_0/n}^{\tilde{T}_c} S^{HBH}(\tilde{T}) d\tilde{T} + \frac{n}{n-1} \xi, \quad (4.1)$$

where ξ is a positive number independent of n . As we mentioned, the inequalities (1.12a) and (1.12d) hold here. To explain the first inequality we can write

$$\frac{\partial}{\partial n} \tilde{S}_n = -\frac{2\pi}{(n-1)^2} \int_{\tilde{T}_0/n}^{\tilde{T}_c} \left[S^{HBH}(\tilde{T}) - S^{HBH}\left(\frac{\tilde{T}_0}{n}\right) \right] d\tilde{T} - \frac{1}{(n-1)^2} \xi. \quad (4.2)$$

The first term is negative because S^{HBH} is a monotonic increasing function of temperature, see $\tilde{S} - \tilde{T}$ diagram in figure 7. Since ξ is a positive constant, the total value of the right hand side of the above expression will be negative.

The fourth inequality can be written in terms of the specific heat

$$\frac{\partial^2}{\partial n^2} ((n-1)\tilde{S}_n) = -\frac{1}{n^2} \left. \frac{\partial \tilde{E}}{\partial \tilde{T}} \right|_{\tilde{T}_0/n}. \quad (4.3)$$

The $\tilde{T} - \tilde{E}$ diagram in figure 7 easily show that the right hand side of the above equation is always negative.

Now let us look at the second inequality (1.12b) which is violated for positive values of coupling λ , as depicted in figure 11. This is completely consistent with the fact that for positive values of coupling there is a temperature where the thermal entropy becomes negative. In fact we have

$$\frac{\partial}{\partial n} \left(\frac{n-1}{n} \tilde{S}_n \right) = \frac{1}{n^2} S^{HBH}\left(\frac{\tilde{T}_0}{n}\right). \quad (4.4)$$

The $\tilde{S} - \tilde{T}$ diagram in figure 7 says that whenever $\frac{\tilde{T}_0}{n}$ is less than a specific temperature the value of thermal entropy becomes negative therefore the second inequality is violated. We

have sketched the violation number n_v in right diagram of figure 12 for positive values of coupling. In fact this violation never happens for $\lambda \leq 0$ because as we see from equation (3.23) for negative values of coupling the thermal entropy is always positive.

The third inequality (1.12c) has a more complicated form

$$\frac{\partial}{\partial n}((n-1)\tilde{S}_n) = 2\pi \int_{\tilde{T}_0/n}^{\tilde{T}_c} S^{HBH}(\tilde{T})d\tilde{T} + \frac{1}{n}\tilde{S}^{HBH}(\frac{\tilde{T}_0}{n}) + \xi. \quad (4.5)$$

The first and second terms above may be positive or negative depending on the value of $\frac{\tilde{T}_0}{n}$ but the last term is always positive. Therefore it will be difficult to find the total sign of the above expression otherwise we use the numerical data. Our numerical analysis shows that this inequality holds in most areas of parameters of the theory as depicted in figure 11.

By numerical analysis for other values of $\Delta_+ > 2$ we conclude that the above arguments are independent of Δ_+ , see figure 12.

Acknowledgment

This work is supported by Ferdowsi University of Mashhad under the grant 3/42540 (1395/10/28). A. G. would like to thank M. Roshan and K. Javidan for valuable discussions on numerical methods. S. Q. would like to thank J. E. Santos for useful discussion.

References

- [1] S. Abramsky and B. Coecke, *Physical Traces: Quantum vs. Classical Information Processing*, [arXiv:cs/0207057v2].
- [2] P. Calabrese and J. L. Cardy, “Entanglement entropy and quantum field theory,” *J. Stat. Mech.* **0406**, P06002 (2004) [hep-th/0405152].
- [3] A. Hamma, R. Ionicioiu and P. Zanardi, *Ground State Entanglement and Geometric Entropy in the Kitaev’s Model*, *Phys. Lett. A* **337** (2005) 22 [arXiv:quant-ph/0406202].
- [4] P. Calabrese and J. L. Cardy, “Entanglement entropy and quantum field theory: A Non-technical introduction,” *Int. J. Quant. Inf.* **4**, 429 (2006) [quant-ph/0505193].
- [5] A. Kitaev and J. Preskill, “Topological entanglement entropy,” *Phys. Rev. Lett.* **96**, 110404 (2006) [hep-th/0510092].
- [6] S. Ryu and T. Takayanagi, “Holographic derivation of entanglement entropy from AdS/CFT,” *Phys. Rev. Lett.* **96**, 181602 (2006) [hep-th/0603001].
- [7] S. Ryu and T. Takayanagi, “Aspects of Holographic Entanglement Entropy,” *JHEP* **0608**, 045 (2006) [hep-th/0605073].
- [8] T. Nishioka, S. Ryu and T. Takayanagi, “Holographic Entanglement Entropy: An Overview,” *J. Phys. A* **42**, 504008 (2009) [arXiv:0905.0932 [hep-th]].
- [9] M. Van Raamsdonk, “Comments on quantum gravity and entanglement,” [arXiv:0907.2939 [hep-th]].

- [10] M. Van Raamsdonk, “Building up spacetime with quantum entanglement,” *Gen. Rel. Grav.* **42**, 2323 (2010) [*Int. J. Mod. Phys. D* **19**, 2429 (2010)] [arXiv:1005.3035 [hep-th]].
- [11] T. Takayanagi, “Entanglement Entropy from a Holographic Viewpoint,” *Class. Quant. Grav.* **29**, 153001 (2012) [arXiv:1204.2450 [gr-qc]].
- [12] E. Bianchi and R. C. Myers, “On the Architecture of Spacetime Geometry,” *Class. Quant. Grav.* **31**, 214002 (2014) [arXiv:1212.5183 [hep-th]].
- [13] R. C. Myers, R. Pourhasan and M. Smolkin, “On Spacetime Entanglement,” *JHEP* **1306**, 013 (2013) [arXiv:1304.2030 [hep-th]].
- [14] V. Balasubramanian, B. Czech, B. D. Chowdhury and J. de Boer, “The entropy of a hole in spacetime,” *JHEP* **1310**, 220 (2013) [arXiv:1305.0856 [hep-th]].
- [15] A. Rényi, “On measures of information and entropy,” in *Proceedings of the 4th Berkeley Symposium on Mathematics, Statistics and Probability*, **1**, 547 (U. of California Press, Berkeley, CA, 1961); A. Rényi, “On the foundations of information theory,” *Rev. Int. Stat. Inst.* **33** (1965) 1.
- [16] H. Li and F. D. M. Haldane, “Entanglement Spectrum as a Generalization of Entanglement Entropy: Identification of Topological Order in Non-Abelian Fractional Quantum Hall Effect States” *Phys. Rev. Lett.* **101**, 010504 (2008) [arXiv:0805.0332]
- [17] J. L. Cardy, O. A. Castro-Alvaredo and B. Doyon, “Form factors of branch-point twist fields in quantum integrable models and entanglement entropy,” *J. Statist. Phys.* **130**, 129 (2008) [arXiv:0706.3384 [hep-th]].
- [18] T. Nishioka and T. Takayanagi, “AdS Bubbles, Entropy and Closed String Tachyons,” *JHEP* **0701**, 090 (2007) [hep-th/0611035].
- [19] A. Velytsky, “Entanglement entropy in d+1 SU(N) gauge theory,” *Phys. Rev. D* **77**, 085021 (2008) [arXiv:0801.4111 [hep-th]].
- [20] P. V. Buividovich and M. I. Polikarpov, “Numerical study of entanglement entropy in SU(2) lattice gauge theory,” *Nucl. Phys. B* **802**, 458 (2008) [arXiv:0802.4247 [hep-lat]].
- [21] H. Casini, M. Huerta and R. C. Myers, “Towards a derivation of holographic entanglement entropy,” *JHEP* **1105**, 036 (2011) [arXiv:1102.0440 [hep-th]].
- [22] S. Aminneborg, I. Bengtsson, S. Holst and P. Peldan, “Making anti-de Sitter black holes,” *Class. Quant. Grav.* **13**, 2707 (1996) [gr-qc/9604005].
- [23] D. R. Brill, J. Louko and P. Peldan, “Thermodynamics of (3+1)-dimensional black holes with toroidal or higher genus horizons,” *Phys. Rev. D* **56**, 3600 (1997) [gr-qc/9705012].
- [24] L. Vanzo, “Black holes with unusual topology,” *Phys. Rev. D* **56**, 6475 (1997) [gr-qc/9705004].
- [25] R. B. Mann, “Pair production of topological anti-de Sitter black holes,” *Class. Quant. Grav.* **14**, L109 (1997) [gr-qc/9607071].

- [26] D. Birmingham, “Topological black holes in Anti-de Sitter space,” *Class. Quant. Grav.* **16**, 1197 (1999) [hep-th/9808032].
- [27] R. Emparan, “AdS membranes wrapped on surfaces of arbitrary genus,” *Phys. Lett. B* **432**, 74 (1998) [hep-th/9804031].
- [28] R. M. Wald, “Black hole entropy is the Noether charge,” *Phys. Rev. D* **48**, no. 8, R3427 (1993) [gr-qc/9307038].
- [29] V. Iyer and R. M. Wald, “Some properties of Noether charge and a proposal for dynamical black hole entropy,” *Phys. Rev. D* **50**, 846 (1994) [gr-qc/9403028].
- [30] L. Y. Hung, R. C. Myers, M. Smolkin and A. Yale, “Holographic Calculations of Renyi Entropy,” *JHEP* **1112**, 047 (2011) [arXiv:1110.1084 [hep-th]].
- [31] P. Caputa, G. Mandal and R. Sinha, “Dynamical entanglement entropy with angular momentum and U(1) charge,” *JHEP* **1311**, 052 (2013) [arXiv:1306.4974 [hep-th]].
- [32] A. Belin, L. Y. Hung, A. Maloney, S. Matsuura, R. C. Myers and T. Sierens, “Holographic Charged Renyi Entropies,” *JHEP* **1312**, 059 (2013) [arXiv:1310.4180 [hep-th]].
- [33] G. Pastras and D. Manolopoulos, “Charged Rnyi entropies in CFTs with Einstein-Gauss-Bonnet holographic duals,” *JHEP* **1411**, 007 (2014) [arXiv:1404.1309 [hep-th]].
- [34] G. Pastras and D. Manolopoulos, “Holographic Calculation of Renyi Entropies and Restrictions on Higher Derivative Terms,” *PoS CORFU 2014*, 157 (2015) [arXiv:1507.08595 [hep-th]].
- [35] K. Zyczkowski, “Rényi extrapolation of Shannon entropy,” *Open Syst. Inf. Dyn.* **10**, 297 (2003) [arXiv:quant-ph/0305062].
- [36] Y. Nakaguchi and T. Nishioka, “A holographic proof of Rnyi entropic inequalities,” *JHEP* **1612**, 129 (2016) [arXiv:1606.08443 [hep-th]].
- [37] A. Belin, A. Maloney and S. Matsuura, “Holographic Phases of Renyi Entropies,” *JHEP* **1312**, 050 (2013) [arXiv:1306.2640 [hep-th]].
- [38] S. A. Hartnoll, C. P. Herzog and G. T. Horowitz, “Holographic Superconductors,” *JHEP* **0812**, 015 (2008) [arXiv:0810.1563 [hep-th]].
- [39] G. T. Horowitz, “Introduction to Holographic Superconductors,” *Lect. Notes Phys.* **828**, 313 (2011) [arXiv:1002.1722 [hep-th]].
- [40] O. J. C. Dias, R. Monteiro, H. S. Reall and J. E. Santos, “A Scalar field condensation instability of rotating anti-de Sitter black holes,” *JHEP* **1011**, 036 (2010) [arXiv:1007.3745 [hep-th]].
- [41] A. Ashtekar and S. Das, “Asymptotically Anti-de Sitter space-times: Conserved quantities,” *Class. Quant. Grav.* **17**, L17 (2000) [hep-th/9911230].

- [42] P. Breitenlohner and D. Z. Freedman, “Stability In Gauged Extended Supergravity,” *Annals Phys.* **144** (1982) 249;
P. Breitenlohner and D. Z. Freedman, “Positive Energy In Anti-De Sitter Backgrounds And Gauged Extended Supergravity,” *Phys. Lett. B* **115** (1982) 197.
- [43] L. Mezincescu and P. K. Townsend, “Stability At A Local Maximum In Higher Dimensional Anti-De Sitter Space And Applications To Supergravity,” *Annals Phys.* **160** (1985) 406.
- [44] A. Buchel, J. Escobedo, R. C. Myers, M. F. Paulos, A. Sinha and M. Smolkin, “Holographic GB gravity in arbitrary dimensions,” *JHEP* **1003**, 111 (2010) [[arXiv:0911.4257](https://arxiv.org/abs/0911.4257) [hep-th]].